碳纳米材料互连线的单粒子串扰特性研究

刘保军[1],张 爽[1],李 成[2]
(1. 空军工程大学航空机务士官学校,河南信阳 464000;
2. 国防科技大学计算机学院高性能计算国家重点实验室,湖南长沙 410073)

摘 要: 碳纳米材料互连线由于其良好的电学、热学和力学特性,成为研究热点. 随着技术节点的缩减,串扰效应对电路的影响愈加显著. 本文针对单壁碳纳米管束(Single Walled Carbon Nanotube Bundles,SWCNT)、多壁碳纳米管束(Multi Walled Carbon Nanotube Bundles,MWCNT)、单层石墨烯(Single Layer Graphene Nano-Ribbon,SLGNR)及多层石墨烯(Multi Layer Graphene Nano-Ribbon,MGLNR)的互连线,研究了统一的等效RLC模型,并构建了单粒子串扰(SEC)的等效电路,对比分析了四种互连线在32 nm,21 nm和14 nm技术节点下的SEC峰值电压和脉冲宽度. 结果表明,与铜互连线相比,碳纳米材料互连线的SEC较弱,但对传输信号的衰减作用较大,综合信号衰减和耦合作用程度,SWCNT和MLGNR更能有效抑制SEC的传播和影响. 最后,本文利用灰色理论,分析了SEC与RLC参数之间的潜在关联性.

关键词: 碳纳米管;石墨烯;互连线;单粒子串扰
基金项目: 国家自然科学基金(No.11975311,No.11405270)
中图分类号: TN406;TN405.97 **文献标识码:** A **文章编号:** 0372-2112(2023)06-1637-07
电子学报URL:http://www.ejournal.org.cn **DOI:**10.12263/DZXB.20210582

Reseach on Single Event Crosstalk Characteristic of Carbon Nanomaterial Interconnects

LIU Bao-jun[1], ZHANG Shuang[1], LI Cheng[2]
(1. *Aviation Maintenance NCO Academy, Air Force Engineering University, Xinyang, Henan* 464000, *China*;
2. *Institute for Quantum Information & State Key Laboratory of High Performance Computing, College of Computer, National University of Defense Technology, Changsha, Hunan* 410073, *China*)

Abstract: Due to its well electrical, thermal and mechanical properties, carbon nanomaterial interconnect has become a research hotspot. As devices feature sizes scale down into nano meter, single event transient (SET) becomes the most serious threat for the reliability of integrated circuits (ICs) with advanced process in the future, which should be highly concerned. With CMOS technology scaling continuing and operating frequencies increasing, SET might bring noise into electronically unrelated multiple logic circuit paths due to increased crosstalk effects between interconnects, which can intensify the SET susceptibility of nanometer CMOS circuits. Therefore, single event crosstalk (SEC) effects should be considered carefully in the early design stages of circuits applied for space and ground radiation environments. As technology nodes scaled down, the impact of crosstalk effects on the integrated circuits becomes more and more significant. Although many works have been carried out on the crosstalk effect of carbon nanomaterial interconnects, the conclusions obtained cannot well guide the analysis and research of the radiation effect of integrated circuits of carbon nanomaterial interconnects. For single-walled carbon nanotube bundles (SWCNT), multi-walled carbon nanotube bundles (MWCNT), single-layer graphene (SLGNR) and multilayer graphene (MGLNR) interconnects, a unified equivalent RLC model is studied. The equivalent circuit of single event crosstalk (SEC) is built. The SEC peak voltage and pulse width of four interconnects at 32 nm, 21 nm and 14 nm technology nodes are compared and analyzed. The results show that, compared with the copper interconnect, the SEC of the carbon nanomaterial interconnects is smaller, but has a greater attenuation effect on the transmission signal. This results in a lower peak voltage and a larger pulse width of SEC. With the technology node scaling down from 32 nm to 14 nm, the peak voltage of SEC tends to increase, and the pulse width of SEC changes insignificantly, except for SWCNT and MLGNR. The peak voltage of SEC in SWCNT interconnect is increased by 2.88 times and the pulse width is reduced by 1.56 times. The peak voltage of SEC in MLGNR is very low, and the pulse width is higher, and almost un-

收稿日期:2021-05-07;修回日期:2021-08-10;责任编辑:王天慧

changed. Comprehensive signal attenuation and coupling degree, the performance of SWCNT and MLGNR is better. They can effectively suppress the propagation and influence of crosstalk. Finally, using grey theory, the potential correlation between SEC and RLC parameters is analyzed. The results show that the coupling capacitance and distributed inductance of interconnects will affect the peak voltage and pulse width to a large extent. Therefore, in the early stage of the circuit design, it is necessary to consider how to layout to reduce the coupling capacitance and inductance, thereby reducing crosstalk noise. These results will provide technical supports and ideas for the optimal design and evaluation of carbon nano interconnects applications in radiation dedicated circuits.

Key words: carbon nanotube; graphene; interconnect; single event crosstalk

Foundation Item(s): National Natural Science Foundation of China (No.11975311, No.11405270)

1 引言

随着器件特征尺寸进入纳米尺度,传统铜互连线电阻率过大等问题愈发严重. 新型的碳纳米材料,如碳纳米管、石墨烯等[1,2],具有良好的电学、热学和力学特性,被认为是很有潜力的互连材料. 同时,互连线的间隔宽度比缩小、厚宽比增加,导致互连线间的耦合效应增强. 故在先进电路芯片设计流水线和信号完整性分析的早期阶段,必须考虑互连线间串扰效应的影响[3,4].

在辐射环境中,高能粒子会诱发单粒子瞬态(Single Event Transient,SET),形成软错误. SET已成为纳米工艺电路须重点关注的辐射效应. 串扰效应可使SET影响不相关路径的电路,从而增加其SET易受攻击部分和敏感性. 故单粒子串扰(Single Event Crosstalk,SEC)的分析和预测是一项非常重要的研究工作[5,6].

针对串扰效应,研究人员已开展了大量工作,如用时域有限差分法、ABCD矩阵法、谱域随机法等进行串扰的预测、延时估计等[7~10],分析温度、频率等对串扰的影响等[11~15]. 针对SEC,Balasubramanian等[16]利用90 nm的单个和两个光子激光吸收技术,测试并证实了SEC的存在;Sayil等[3,6]基于互连线的4-π分布RC网络模型,提出了一种SEC预测模型,平均误差约6.16%,并分析了温度的影响;Liu等[4,17,18]基于导纳规则,建立了SEC的估计模型,平均误差3.07%,并建立了多线间SEC的预测模型,平均误差5.52%;综合考虑寄生容性和感性效应,构建了SEC解析模型,预测误差为2.19%. 以上研究均是针对铜互连线的,尚缺乏新型碳纳米材料互连线的SEC的相关研究. 虽然研究人员针对碳纳米材料互连的串扰效应开展了一些研究,但系统性不强,得到的结论并不能很好地指导集成电路的辐射效应分析和研究. 因此,迫切需要开展新型碳纳米材料互连线的SEC相关研究.

2 互连线的等效RLC模型

本文碳纳米材料互连线是金属性的,主要考虑四种类型[1,2,7~9,12,13,19~22]:单壁碳纳米管束(Single Walled Carbon Nanotube bundle,SWCNT)、多壁碳纳米管束(Multi-Walled Carbon Nanotube bundle,MWCNT)、单层石墨烯(Single Layer Graphene Nano-Ribbon,SLGNR)及多层石墨烯(MultiLayer Graphene Nano-Ribbon,MLGNR),如图1所示. 其中,w,h,l分别表示互连线的宽度、厚度和长度,s是两线间隔,h_t是距地面高度,互连线与地面之间是介质材料,D是单壁碳纳米管直径,$D_{\min}$和$D_{\max}$分别是多壁碳纳米管的最小和最大直径,δ=0.34 nm是范德华距离.

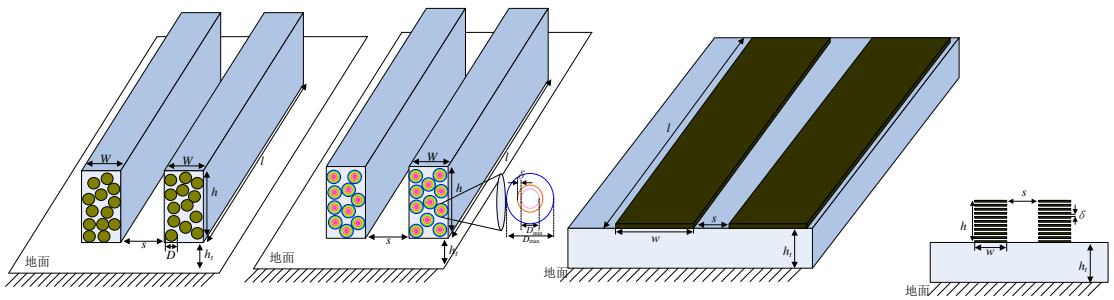

(a) SWCNT (b) MWCNT (c) SLGNR (d) MLGNR

图1 碳纳米材料互连线结构示意图

这里将碳纳米互连线等效为单导体(Equivalent Single Conductor,ESC),即将其各方面的影响都转化为电阻、电容和电感三种参数来考量,同时,考虑到各参数的影响因素的不同,提取的等效电路参数分为集总和分布参数两类[2,7,12,19]. 图2为提取的碳纳米材料互连线的等效RLC电路模型,其中,R_c,R_q分别为集总的接触电阻和量子电阻,r_s,l_k,l_m,c_q,c_e均是分布式参数,分别表示散射电阻、动态电感、磁性电感、量子电容及静电电容.

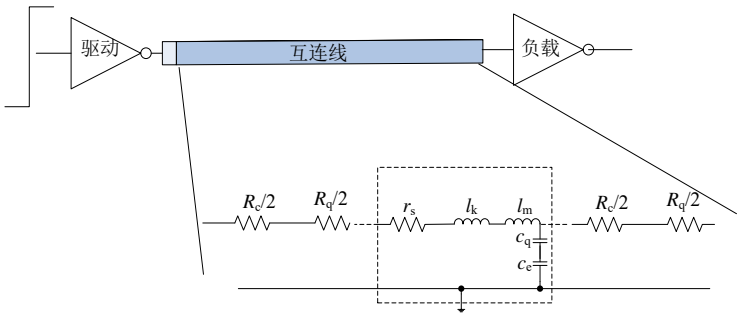

图2　互连线的等效RLC模型

下面分析四种碳纳米材料互连线等效RLC模型中的参数,接触电阻与互连线的材料有很大关系,其值在几百到上千欧之间. 通过对四种互连线类型的RLC参数进行归纳总结[1,2,7~9,12,13,19~22],得到了统一的RLC解析模型,如式(1)和表1所示.

$$R_q=\frac{h_B}{2q^2N_{cnt}\sum_{i=1}^{N}N_i} \tag{1a}$$

$$r_s=\frac{h_B}{2q^2N_{cnt}\sum_{i=1}^{N}N_i\lambda_i(T)} \tag{1b}$$

$$l_k=\frac{h_B}{4q^2v_FN_{cnt}\sum_{i=1}^{N}N_i} \tag{1c}$$

$$l_m=\frac{\mu_0}{2\pi}g(w,h_t) \tag{1d}$$

$$c_q=\frac{4q^2}{h_Bv_F}N_x \tag{1e}$$

$$c_e=\varepsilon_0\varepsilon_r f(w,h_t) \tag{1f}$$

其中,h_B是普朗克常数,其值为6.625×10^{-34} J·s,q是电子电荷,为1.602×10^{-19} C,v_F是费米速度,为8×10^5 m/s,μ_0是真空磁导率,为$4\pi\times10^{-7}$ H/m,ε_0是真空的介电常数,为8.854×10^{-12} F/m,ε_r是介质的相对介电常数.

表1　式(1)中的相关参数

参数	互连线类型			
	SWCNT	MWCNT	SLGNR	MLGNR
N_{cnt}	$N_w=\lfloor(w-D)/(D+\delta)\rfloor+1\quad N_H=\lfloor 2/\sqrt{3}\times(h-D)/(D+\delta)\rfloor+1 N_{cnt}=P_m(N_HN_w-\lfloor N_H/2\rfloor)$		1	$\lfloor h/\delta\rfloor+1$
N	1	$\lfloor(D_{max}-D_{min})/(2\delta)\rfloor+1$	1	
N_i	2	$N_i=\begin{cases}aTD_i+b, & D_i>d_T/T\\ 2/3, & D_i>d_T/T\end{cases}$	$\alpha E_F w$	
$\lambda_i(T)$	$\lambda_i(T)=(\lambda_{AC}^{-1}+\lambda_{op,ems}^{-1}+\lambda_{op,abs}^{-1})^{-1},\ \lambda_{op,ems}(T)=\left[\lambda_{op,ems}^{fd}(T)^{-1}+\lambda_{op,ems}^{abs}(T)^{-1}\right]^{-1}$ $\lambda_{op,ems}^{abs}(T)=\lambda_{op,abs}+\lambda_{op},\ \lambda_{op,ems}^{fd}(T)=y(T)l/V_{DD}+\lambda_{op},\ N_{OP}(T)=\frac{1}{\exp(\frac{h_{B.op}}{k_BT})-1}$			
	$\lambda_{AC}=1\,600\times(\frac{300}{T})$ $\lambda_{op}=15\times\frac{N_{OP}(300)+1}{N_{OP}(T)+1}$ $\lambda_{op,abs}=15\times\frac{N_{OP}(300)+1}{N_{OP}(T)}$ $y(T)=\frac{h_{B.op}}{q}$	$\lambda_{AC}=\frac{4\times10^5D_i}{T}$ $\lambda_{op}=56D_i\frac{N_{OP}(300)+1}{N_{OP}(T)+1}$ $\lambda_{op,abs}=e^{\frac{h_{B.op}}{k_BT}}\lambda_{op}$ $y(T)=\frac{h_{B.op}-k_BT}{q}$	$\lambda_{AC}=\frac{\rho_m(h_B/\pi v_Fv_s)^2}{\sqrt{\pi N_s}D_{AC}^2k_BT}$ $\lambda_{op,abs}=\frac{\rho_mh_{B.op}v_F^2}{\sqrt{\pi N_s}D_{op}^2N_{OP}(1+\frac{2\pi h_{B.op}}{h_Bv_F\sqrt{\pi N_s}})}$ $\lambda_{op,ems}=\frac{\rho_mh_{B.op}v_F^2}{\sqrt{\pi N_s}D_{op}^2N_{OP}(1-\frac{2\pi h_{B.op}}{h_Bv_F\sqrt{\pi N_s}})}$	
$g(w,h_t)$	$\frac{1}{N_w}\cosh^{-1}(\frac{D+2h_t}{D})$		$\cosh^{-1}(\frac{h_t}{w})$	$\frac{2\pi h_t}{w}$
N_x	$N_{cnt}\sum_{i=1}^{N}N_i$			$\frac{1}{2}\alpha wE_F(1+\sqrt{1+1/\alpha\beta E_F})$
$f(w,h_t)$	$\frac{2\pi N_w}{\cosh^{-1}(\frac{D+2h_t}{D})}$		$M(\tanh(\frac{\pi w}{h_t}))$	$\frac{w}{h_t}$

表1中未加说明的D均指最大直径，MLGNR的动态电感l_k需利用迭代的方法得到[1]，k_B是玻尔兹曼常数，为 1.38×10^{-23} J/K，a=2.04×10^{-4} nm$^{-1}\cdot$K^{-1}，b=0.425，d_T=1 300 nm·K，α=1.2 eV$^{-1}\cdot$nm^{-1}，β=2.3 nm，$h_{B.op}$=0.18 eV，ρ_m=7.6×10^{-7} kg/m^2，v_s=20 km/s，N_s=4×10^{16} m^2，D_{AC}=8 eV，D_{op}=2×10^{11} eV/m，$\lfloor\cdot\rfloor$表示向下取整，N_{cnt}是导电管(层)数，N是单根(层)导线的导电沟道数，$\lambda_i(T)$是温度为T时，第i个导电沟道中的电子平均自由程，D_i是单根MWCNT第i层的直径，P_m是导线管束中金属性碳纳米管的比例，E_F是费米能级，V_{DD}是加载电压，$M(x)$是一个分段函数，表达式如下：

$$M(x)=\begin{cases}2\pi\left[\ln\left(2\times\dfrac{1+\sqrt[4]{1-x^2}}{1-\sqrt[4]{1-x^2}}\right)\right]^{-1}, & 0\leqslant x<\dfrac{1}{\sqrt{2}}\\ \dfrac{2}{\pi}\ln\left(2\times\dfrac{1+\sqrt{x}}{1-\sqrt{x}}\right), & \dfrac{1}{\sqrt{2}}\leqslant x\leqslant 1\end{cases}\tag{2}$$

3 SEC等效电路

高能粒子诱发的SET，在电路分析中通常采用在敏感结点引入瞬态双指数电流源来表征[4]，表达式为

$$I(t)=\frac{Q_{dep}}{\tau_\alpha-\tau_\beta}\left(e^{-t/\tau_\alpha}-e^{-t/\tau_\beta}\right)\tag{3}$$

其中，Q_{dep}是粒子入射的累积电荷量，τ_α是p-n结的电荷收集时间常数，τ_β是粒子轨迹初始化建立的时间常数．这里的τ_α和τ_β分别设置为50 ps和1 ps.

针对反相器链，通过两根耦合碳纳米材料互连线来分析SEC，原始电路图如图3(a)所示．将互连线等效为RLC的分布式网络(图2)，驱动反相器缓冲端等效为RC并联网络，负载端等效为电容，施扰线加载SET瞬态电流源，受扰线保持静止，构建的SEC等效电路如图3(b)所示，基于ESC和保角变换方法得到耦合电容c_c和耦合电感l_M的表达式[12,19,20,22]，如式(4)所示，式中耦合电容和电感的上标分别对应SWCNT，MWCNT，SLGNR和MLGNR等四种互连线的耦合电容和电感．

$$c_c^{SWCNT}=\frac{N_w-2}{2}\frac{2\pi\varepsilon_0\varepsilon_r}{\ln\left(\dfrac{s+w}{D}\right)}+\frac{3N_H+4}{5}\frac{2\pi\varepsilon_0\varepsilon_r}{\ln\left(\dfrac{s}{D}\right)}\tag{4a}$$

$$c_c^{MWCNT}=\frac{\pi\varepsilon_0\varepsilon_r N_{cnt}}{\ln\left(\dfrac{s}{D_{max}}+\sqrt{\left(\dfrac{s}{D_{max}}\right)^2+1}\right)}\tag{4b}$$

$$c_c^{SLGNR}=\frac{\varepsilon_0\varepsilon_r}{4}M\left(\sqrt{1-(1+2w/s)^{-2}}\right)\tag{4c}$$

$$c_c^{MLGNR}=\left(\frac{0.5}{1+s^2/(h_t+h)^2}C_{[BCP]}\left(\frac{h}{s/2},\frac{2d}{s/2}\right)+\frac{0.87}{1+(s/2)^2/(h_t+h)^2}C_{[CP]}(w/s)\right)\tag{4d}$$

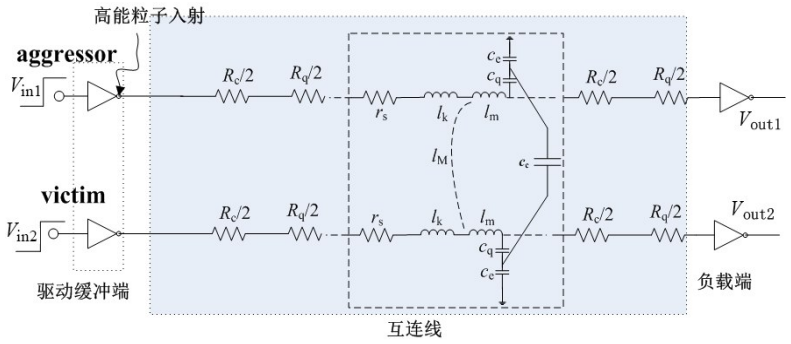

(a) 原始电路

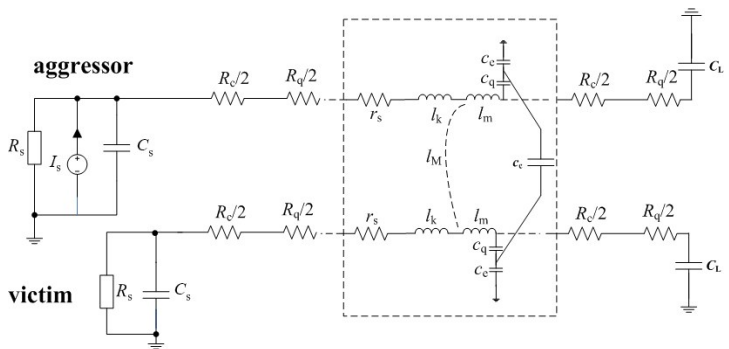

(b) 等效电路

图3 SEC等效电路

$$l_{\mathrm{M}}^{\mathrm{SWCNT/MWCNT}}=\frac{1}{N_{\mathrm{H}}}\frac{\mu_0}{2\pi}\left[\ln\left(\frac{l}{s+D}+\sqrt{1+\left(\frac{l}{s+D}\right)^2}\right)+\frac{s+D}{l}-\sqrt{1+\left(\frac{s+D}{l}\right)^2}\right] \tag{4e}$$

$$l_{\mathrm{M}}^{\mathrm{MLGNR}}=\frac{\mu_0}{2\pi}l\left[\ln\left(\frac{l}{s+w}+\sqrt{1+\left(\frac{l}{s+w}\right)^2}\right)+\frac{s+w}{l}-\sqrt{1+\left(\frac{s+w}{l}\right)^2}\right] \tag{4f}$$

其中,SLGNR 的 l_{M} 忽略不计,函数 $C_{[\mathrm{BCP}]}(z,y)$ 和 $C_{[\mathrm{CP}]}(x)$ 见文献[22].

4　仿真与分析

针对四种碳纳米材料互连线系统,设置技术节点分别为32 nm,21 nm和14 nm,互连线为全局型,相关参数设置参考ITRS-2013. 为了对比分析性能,同时仿真了同技术节点下的铜互连的RLC分布模型[23],并考虑了纳米尺度下铜电阻率的变化[1].

下面是SEC脉冲宽度和峰值电压的定义[24]. 设高能粒子作用下,负载端得到的输出电压为 $V_{\mathrm{out}}(t)$,则有效脉冲宽度为

$$W_{\mathrm{SEC}}=\frac{\int_0^{\infty}tV_{\mathrm{out}}(t)\mathrm{d}t}{\int_0^{\infty}V_{\mathrm{out}}(t)\mathrm{d}t} \tag{5}$$

峰值电压为

$$V_{\mathrm{peak}}=\frac{\int_0^{\infty}V_{\mathrm{out}}(t)\mathrm{d}t}{W_{\mathrm{SEC}}}=\frac{\left(\int_0^{\infty}V_{\mathrm{out}}(t)\mathrm{d}t\right)^2}{\int_0^{\infty}tV_{\mathrm{out}}(t)\mathrm{d}t} \tag{6}$$

随着器件特征尺寸的不断缩减,很小的累积电荷(几fC)也可诱发显著的瞬态电流. 设置粒子入射的累积电荷量为9.8fC,互连线的长度为200 μm,利用SPICE仿真SEC电路,通过式(5)和式(6)计算不同技术节点、不同互连线类型的SEC峰值电压和脉冲宽度,结果如图4和表2所示.

表2　不同互连线的SEC的传输系数

互连线类型		施扰线远端/施扰线近端		受扰线远端/施扰线远端	
		峰值电压	脉冲宽度	峰值电压	脉冲宽度
Cu	32 nm	0.936 9	1.064 1	0.611 0	1.158 5
	21 nm	0.856 8	1.155 6	0.659 9	1.127 2
	14 nm	0.597 9	1.584 7	0.759 0	1.067 3
SWCNT	32 nm	0.934 1	1.053 3	0.634 6	0.697 8
	21 nm	0.890 7	1.084 3	0.600 3	0.695 8
	14 nm	0.756 0	1.190 2	0.697 2	0.804 9
MWCNT	32 nm	0.730 8	1.305 9	0.879 2	1.045 3
	21 nm	0.726 9	1.317 0	0.843 0	1.058 4
	14 nm	0.432 7	1.988 1	0.954 8	1.012 5
SLGNR	32 nm	0.168 9	5.870 1	0.266 2	1.233 9
	21 nm	0.162 6	6.069 5	0.244 8	1.207 5
	14 nm	0.140 0	7.057 5	0.295 2	1.216 0
MLGNR	32 nm	0.894 0	1.088 6	0.040 5	0.616 8
	21 nm	0.846 1	1.130 5	0.033 2	0.635 0
	14 nm	0.775 2	1.233 8	0.042 4	0.659 6

由图4可见,与铜互连线相比,碳纳米材料互连线的SEC峰值电压较低,而脉冲宽度则偏高,且随着技术节点的缩减,SEC峰值电压呈增加趋势,而脉冲宽度变化不显著. 但SWCNT和MLGNR是例外. 当技术节点从32 nm缩减到14 nm时,SWCNT的峰值电压增加2.88倍、脉冲宽度减少1.56倍,MLGNR的峰值电压非常低,脉冲宽度比较高,且几乎无变化,其原因是SWCNT的耦合电容变化显著,而MLGNR的 c_{c} 变化不显著. 由表2可知,随着技术节点的缩减,互连线的阻抗增加,对信号传输的衰减作用增强,导致施扰线远端与其近端的峰值电压

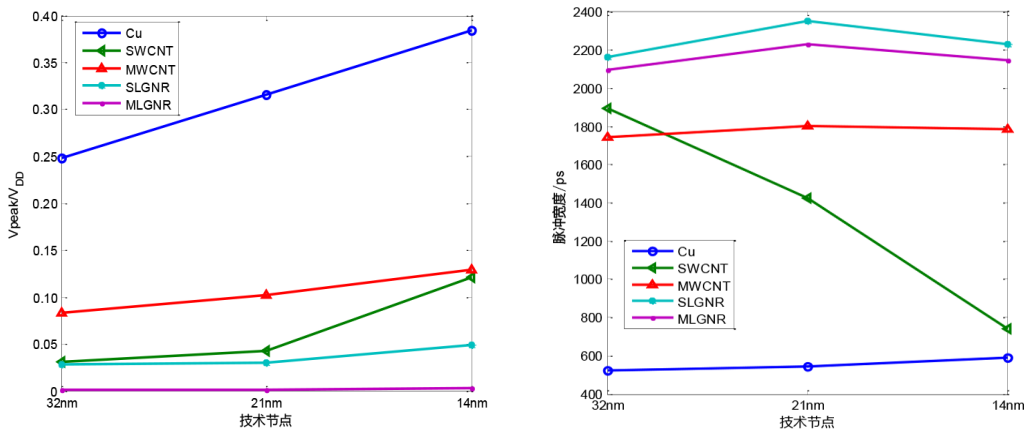

(a)峰值电压　　(b)脉冲宽度

图4　不同技术节点、不同互连线类型的SEC

比值呈显著减小趋势，但SLGNR和MLGNR的峰值电压比值变化相对较小，同时，较长的SLGNR传播信号时，对信号的衰减作用较为严重，故其并不适合作为长互连线来传输信号. 结合受扰线与施扰线远端的峰值电压比值来看，两线间的耦合程度由高到低为MWCNT, Cu, SWCNT, SLGNR, MLGNR. 因此，由于SLGNR和MWCNT的信号衰减作用较强，结合耦合程度的差异，最终导致图4中的SWCNT, SLGNR及MLGNR的峰值电压偏低. 对于脉冲宽度而言，信号在互连线的传播，均会一定程度地展宽脉冲，但SWCNT和MLGNR的耦合程度相对较低，串扰脉宽比值偏小. 综合信号的衰减程度和耦合效应，SWCNT和MLGNR更能有效抑制串扰的传播和影响.

为了深入分析SEC等效电路中RLC参数(图2)，与峰值电压及脉冲宽度之间的潜在关联性，设置不同技术节点、不同互连线长度，获取相应的峰值电压和脉冲宽度，利用灰色理论[25]，计算它们的综合关联度，分析潜在的关联性，结果如表3所示.

表3 互连线RLC参数与SEC间的灰色综合关联度

参数		R_c+R_q	r_s	l_k+l_m	$c_ec_q/(c_e+c_q)$	c_c	l_M
峰值电压	32 nm	0.760 1	0.849 9	**0.866 8**	**0.990 1**	**0.932 2**	0.602 2
	21 nm	0.761 9	0.837 1	**0.858 0**	**0.987 3**	**0.928 4**	0.599 6
	14 nm	0.769 0	0.820 8	**0.845 0**	**0.911 9**	**0.937 8**	0.588 1
脉冲宽度	32 nm	0.756 8	**0.926 4**	**0.956 1**	0.886 2	**0.944 1**	0.602 3
	21 nm	0.757 2	**0.922 4**	**0.963 4**	0.883 1	**0.927 0**	0.599 6
	14 nm	0.759 1	**0.898 7**	**0.949 2**	0.827 2	**0.908 3**	0.588 2

由表可知，峰值电压与分布电感(l_k+l_m)、电容($c_ec_q/(c_e+c_q)$)和耦合电容(c_c)之间存在较高的关联，脉冲宽度与分布电阻(r_s)、电感(l_k+l_m)和耦合电容(c_c)之间存在较高的关联，且关联程度随技术节点的缩减呈减小趋势，而峰值电压和脉冲宽度，与互感(l_M)及集总电阻(R_c+R_q)的关联程度偏弱. 综合上述分析，耦合电容和分布电感在很大程度上会同时影响峰值电压和脉冲宽度，因此，在电路设计时，要考虑如何布局来降低耦合电容及电感，进而达到降低串扰噪声的目的.

5 结论

碳纳米材料互连线具有很好的电学、热学和力学特性，被认为具有潜力应用的互连材料. 随着器件特征尺寸的不断缩减，单粒子瞬态(SET)已成为辐射环境中集成电路软错误的主要来源，严重威胁着电路的可靠性. 不断增强的互连线耦合效应，进一步恶化了SET对电路的影响. 本文对SWCNT, MWCNT, SLGNR和MLGNR等四种新型的碳纳米材料互连线，构建了统一的RLC等效模型及其单粒子串扰(SEC)等效电路模型，通过分析32 nm，21 nm及14 nm技术节点下SEC的峰值电压和脉冲宽度，探讨了四种新型互连线对SEC、信号传输的影响，并基于灰色关联理论，分析了RLC参数与SEC之间潜在的关联性，对比分析了四种碳纳米互连材料的SEC特点，为碳纳米互连线在辐射专用电路中应用的优化设计和评估提供技术支撑和思路.

参考文献

[1] 崔江澎. 碳纳米管及石墨烯在纳米集成电路互连线中的相关研究 [D]. 杭州:浙江大学, 2012.
CUI J P. Some Investigation on Carbon Nanotubes and Grapheme as Interconnect in Nanosacle Integrated Circuits [D]. Hangzhou: Zhejiang University, 2012. (in Chinese)

[2] CUI J P, ZHAO W S, YIN W Y, et al. Signal transmission analysis of multilayer graphene nano-ribbon (MLGNR) interconnects[J]. IEEE Transactions on Electromagnetic Compatibility, 2012, 54(1): 126-132.

[3] SAYIL S, BOORLA V K, YEDDULA S R. Modeling single event crosstalk in nanometer technologies[J]. IEEE Transactions on Nuclear Science, 2011, 58(5): 2493-2502.

[4] LIU B J, CAI L, ZHU J. Accurate analytical model for single event (SE) crosstalk[J]. IEEE Transactions on Nuclear Science, 2012, 59(4): 1621-1627.

[5] ARTOLA L, GAILLARDIN M, HUBERT G, et al. Modeling single event transients in advanced devices and ICs[J]. IEEE Transactions on Nuclear Science, 2015, 62(4): 1528-1539.

[6] SAYIL S, BHOWMIK P. Mitigating the thermally induced single event crosstalk[J]. Analog Integrated Circuits and Signal Processing, 2017, 92: 247-253.

[7] AGRAWAL Y, KUMAR M G, CHANDEL R. Comprehensive model for high-speed current-mode signaling in next generation MWCNT bundle interconnect using FDTD technique[J]. IEEE Transactions on Nanotechnology, 2016, 15(4): 590-598.

[8] SAHOO M, GHOSAL P, RAHAMAN H. Modeling and analysis of crosstalk induced effects in multiwalled carbon nanotube bundle interconnects: An ABCD parameter-based approach[J]. IEEE Transactions on Nanotechnology, 2015, 14: 259-274.

[9] MAJUMDER M K, DAS P K, KAUSHIK B K. Delay and crosstalk reliability issues in mixed MWCNT bundle interconnects[J]. Microelectronics Reliability, 2014, 54: 2570-

2577.

[10] 李 鑫, M Wang Janet, 张 瑛, 等. 工艺随机扰动下非均匀RLC互连线串扰的谱域方法分析[J]. 电子学报, 2009, 37(2): 398-403.
LI X, Janet M W, ZHANG Y, et al. Spectral method for analysis of crosstalk of non-uniform RLC interconnects in the presence of process variations[J]. Chinese Journal of Electronics, 2009, 37(2): 398-403. (in Chinese)

[11] MAJUMDER M K, KUKKAM N R, KAUSHIK B K. Frequency response and bandwidth analysis of multi-layer graphene nanoribbon and multi-walled carbon nanotube interconnects[J]. Micro & Nano Letters, 2014, 9(9): 557-560.

[12] RAI1M K, SARKAR S. Temperature dependant crosstalk analysis in coupled single-walled carbon nanotube (SWCNT) bundle interconnects[J]. International Journal of Circuit Theory and Applications, 2015, 43: 1367-1378.

[13] RAI M K, ARORA S, KAUSHIK B K. Temperature-dependent modeling and performance analysis of coupled MLGNR interconnects[J]. International Journal of Circuit Theory and Applications, 2018, 46: 299-312.

[14] 魏建军, 王振源, 陈付龙, 等. 温度和频率对互连线信号完整性的影响[J]. 哈尔滨工程大学学报, 2019, 40(4): 834-838.
WEI J J, WANG Z Y, CHEN F L, et al. Influence of temperature and frequency on signal integrity in IC interconnects[J]. Journal of Harbin Engineering University, 2019, 40(4): 834-838. (in Chinese)

[15] BAGHERI A, RANJBAR M, HAJI-NASIRI S, et al. Modelling and analysis of crosstalk induced noise effects in bundle SWCNT interconnects and its impact on signal stability[J]. Journal of Computational Electronics, 2017, 16: 845-855.

[16] BALASUBRAMANIAN A, AMUSAN O A, BHUVA B L, et al. Measurement and analysis of interconnect crosstalk due to single events in a 90 nm CMOS technology[J]. IEEE Transactions on Nuclear Science, 2008, 55(4): 2079-2084.

[17] LIU B J, WEI B, ZHANG S,et al. Modeling and analysis single event crosstalk modeling in multi-lines system[C]// IEEE 4th Advanced Information Technology, Electronic and Automation Control Conference. Chengdu: IEEE, 2019: 1928-1932.

[18] LIU B J, CAI L, LIU X Q. An analytic model for predicting single event (SE) crosstalk of nanometer CMOS circuits[J]. Journal of Electronic Testing: Theory and Applications, 2020, 36(8): 461-467.

[19] ZHAO S, PAN Z. Bandwidth expanding technology for dynamic crosstalk aware single-walled and multi-walled carbon nanotube bundle interconnects[J]. Microelectronics Journal, 2018, 78: 101-113.

[20] KHEZELI M R, MOAIYERI M H, JALALI A. Active shielding of MWCNT bundle interconnects: an efficient approach to cancellation of crosstalk-induced functional failures in ternary logic[J]. IEEE Transactions on Electromagnetic Compatibility, 2019, 61(1): 100-110.

[21] 吴纪森. 石墨烯互连线的串扰特性研究 [D]. 西安: 西安电子科技大学, 2015.
WU J S. Study of Crosstalk Characteristic of Grapheme Interconnects [D]. Xi'an: Xidian University, 2015. (in Chinese)

[22] AGRAWAL Y, KUMAR M G, CHANDEL R. A novel unified model for copper and MLGNR interconnects using voltage- and current-mode signaling schemes[J]. IEEE Transactions on Electromagnetic Compatibility, 2017, 59(1): 217-227.

[23] 朱樟明, 钱利波, 杨银堂. 一种基于纳米级CMOS工艺的互连线串扰RLC解析模型[J]. 物理学报,2009, 58(4): 2631-2636.
ZHU Z M, QIAN L B, YANG Y T. A novel interconnect crosstalk RLC analytic model based on the nanometer CMOS technology[J]. Acta Physica Sinica, 2009, 58(4): 2631-2636. (in Chinese)

[24] 李建伟. 考虑工艺波动的互连线模型研究 [D]. 西安: 西安电子科技大学, 2010.
LI J W. Research on Interconnect Model Considering Process Variations[D]. Xi'an: Xidian University, 2010. (in Chinese)

[25] 刘思峰. 灰色系统理论及其应用[M]. 第六版. 北京: 科学出版社, 2013.
LIU S F. Theory and Application of Grey System[M]. 6th edition. Beijing: Science Press, 2013. (in Chinese)

作者简介

刘保军　男,1984年生,山西灵丘人.博士,副教授.主要研究方向为微纳电路系统可靠性、战伤抢修研究.
E-mail: liubaojun102519@sina.com

张　爽　男,1981年生,河南信阳人.副教授.主要研究方向为可靠性研究、飞机战伤抢修理论与技术研究.

李　成　男,1993年生,湖北恩施人.博士研究生.主要研究方向为新型信息器件.